Physics of the Earth and Planetary Interiors 261 (2016) 36–45

Contents lists available at ScienceDirect

Physics of the Earth and Planetary Interiors

journal homepage: www.elsevier.com/locate/pepi

Single slip dynamics

Andrea Bizzarri [a], Alberto Petri [b,*]

[a] Istituto Nazionale di Geofisica e Vulcanologia, Sezione di Bologna, Via Donato Creti 12, I-40128 Bologna, Italy
[b] CNR – Istituto dei Sistemi Complessi, Dipartimento di Fisica, Sapienza Università, Piazzale Aldo Moro 2, I-00185 Roma, Italy

ARTICLE INFO

Article history:
Received 31 July 2015
Received in revised form 2 July 2016
Accepted 7 July 2016
Available online 15 July 2016

Keywords:
Rheology of faults
Dynamic modeling
Numerical algorithms

ABSTRACT

In the present paper we consider a 1-D, single spring-slider analog model of fault and we solve the equation of motion within the coseismic time window. We incorporate in the dynamic problem different rheologic behavior, starting from the Coulomb friction (which postulates a constant value of the dynamic resistance), then the viscous rheology (where the friction resistance linearly depends on the sliding speed), and finally a version of the more refined rate-and state-dependent friction law. We present analytical solutions of the equation of motion for the different cases and we are able to find the common features of the solutions, in terms of the most important physical observables characterizing the solutions of a 1-D dynamic fault problem; the peak slip velocity, the time at which it is attained (or, in other words, the so-called rise time), the total cumulative slip developed at the end of the process (assumed to occur when the sliding speed vanishes or become comparable to its initial value). We also extract some useful dependences of these quantities on the parameters of the models. Finally, we compare the spectral behavior of the resulting sliding velocity and its fall-off at high frequencies.

1. Introduction

In the present paper we consider the coseismic phase of an earthquake event, i.e., the time window during which the stress is released on the fault and the elastic waves are excited by the stress redistribution caused by the dynamic rupture propagation. We adopt the well-known mass-spring dashpot model (reader can refer to the key papers by Gu et al. (1984) and Rice and Tse (1986) for the general understanding of the model, although the related literature is immense) in which the non elastic effects are accounted in the formulation of a specific fault governing model (rheologic constitutive relations). There is no reason to overemphasize the limitations of this intentionally simple analog fault model: (i) all the properties of the fault are assumed to be homogeneous (in other words, we disregard possible frictional heterogeneities and the adopted parameters represent an average of the overall fault properties) and (ii) due to the 1-D nature of the problem (we have only a temporal dependence in the physical observables), there is no the concept of the rupture front, energy flux in the cohesive zone and rupture speed. Despite of these intrinsic limitations, the spring-slider model has been indeed the subject of an incredible large number of studies dealing with the earthquake slow nucleation, earthquake recurrence, stress triggering, etc. (reader can refer to Bizzarri (2012c) and references cited therein for a thorough and general review).

In the present study we assume different friction models; Coulomb friction, viscous friction and a version of the more elaborated and perhaps more realistic rate-and state-dependent (RS therein after) friction law (e.g., Ruina, 1983). Due to the inherent simplicity of the equation of motion for the geometry considered, contrarily to extended fault models, we are able to find analytical solutions (although not in closed for the RS case). Indeed, it is well known that the only configuration in which it is possible to find analytical solutions is represented by the 2-D, purely in-plane, homogeneous, non-spontaneous (i.e., without prior-assigned rupture speed) case (Kostrov, 1974), but they cannot be expressed in a closed-form, in that a very large number of integrals have to be solved numerically, so that the real advantages with respect to a fully numerical solution disappear.

In this study, by comparing the analytical solutions of the 1-D dynamic problem we will understand what RS really add with respect to more simple friction models. We explore the relations between the most prominent observables of a rupture (such as the duration of slip, the peak in slip velocity, their relationship with the stress drop, the spectral decay and the frequency content of the slip velocity). The relations between different observables are important; indeed, one goal of modern-days seismology is to design computationally efficient and robust numerical algorithms

* Corresponding author.
E-mail addresses: andrea.bizzarri@ingv.it (A. Bizzarri), alberto.petri@isc.cnr.it (A. Petri).

http://dx.doi.org/10.1016/j.pepi.2016.07.004
0031-9201/

able to generate a catalog of synthetic events (i.e., to simulate the synthetic motions recorded on the free surface). Investigations about the possible correlations between various dynamic variables can definitively represent an improvement in the design of physics-based models crucial for realistic ground motions simulation and seismic hazard analysis, as well as in that of the kinematic modeling of faults, on which current practice in seismic engineering relies (Bizzarri, 2012b). Slip characteristics, such as the symmetry properties of the velocity function in time, can also be of help in the formulation of general simplified models for slipping (Baldassarri et al., 2003), and in their analysis (Annunziata et al., 2016).

In Table 1 we report all the most relevant quantities used in the present study. In the following sections we will solve the equation of motion for our analog fault model and for different rheologic configurations.

Except when differently specified, for all practical examples we adopt the values in the Tables 2 and 3 (Section 4).

2. Coulomb friction

We consider first a mass of surface density m attached to a harmonic spring of elastic constant, per surface unit, k, subject to Coulomb friction. The mass is initially in $x = 0$ and it is creeping at speed $\dot{x} = v_0$. Let us suppose to stretch the spring at a very slow rate (but still much larger than v_0) in the positive x direction. In the presence of first detachment force τ_u (Coulomb static friction), the mass begins to move when the coordinate of the spring x_L is such that

$$F = kx_L - \tau_u \geqslant 0 \tag{1}$$

that is for

$$x_L = \frac{\tau_u}{k}. \tag{2}$$

Then the equation of motion reads

$$\ddot{x} + \omega_0^2(x - x_L) + \frac{\tau_f}{m} = 0 \tag{3}$$

where $\omega_0 \equiv \sqrt{k/m}$, and τ_f is the dynamic friction which is constant through time in the present case. From Eq. (3) it is clear that we disregard the loading rate term $kv_{load}t$, where v_{load} is the loading (or plate) velocity. This approximation is totally justified, in that within the coseismic phase (accounted in the present study and lasting up to few minutes) the contribution of the loading term is practically null.

Since $kx_L = \tau_u$ (see Eq. (2)), if we introduce the breakdown stress drop $\Delta\tau_b = \tau_u - \tau_f$ (Bizzarri, 2011) we can write the general solution as

$$x(t) = ae^{-i\omega_0 t} + be^{-i\omega_0 t} + \frac{\Delta\tau_b}{m\omega_0^2}.$$

By imposing the initial conditions mentioned above ($x(0) = 0\, \dot{x}(0) = v_0$) one gets

$$x(t) = \frac{\Delta\tau_b}{k}[1 - \cos(\omega_0 t)] + \frac{v_0}{\omega_0}\sin(\omega_0 t) \tag{4}$$

(this solution holds even for $x^+(0)$), and consequently

$$\dot{x}(t) = \omega_0 \frac{\Delta\tau_b}{k}\sin(\omega_0 t) + v_0\cos(\omega_0 t) > 0. \tag{5}$$

Since we do not allow motion reversal, we consider the slip ended when the velocity drops to zero.

From Eqs. (4) and (5) it is straightforward to derive some simple features characterizing the slip, such as its extension s, duration t_f (also known as rise time), the maximum velocity reached during the slip, v_{peak}, and the time t_{peak} at which it is attained. By neglecting v_0 for the sake of simplicity (typical values are around $v_0 = 3.17 \cdot 10^{-10}$ m/s, and therefore negligible with respect typical coseismic values which span from 0.1 to tens of m/s) we obtain:

$$s = \frac{2\Delta\tau_b}{k} \quad t_f = \frac{\pi}{\omega_0}$$
$$v_{peak} = \frac{\omega_0\Delta\tau_b}{k} \quad t_{peak} = \frac{\pi}{2\omega_0}.$$

From the above expressions we can conclude that:

(a) The slip extension, and thus the magnitude of the instability event, does not depend on the mass, and does not change when both spring constant k and $\Delta\tau_b$ increase by a same factor.
(b) The slip velocity function is perfectly symmetric in time with respect to t_{peak}.
(c) The slip duration only depends on ω_0 and is independent of the friction.
(d) The same holds for t_{peak}.

Table 1
Most relevant quantities used in the present paper.

τ_u	Static friction
τ_f	dynamic friction
$\Delta\tau_b$	$\tau_u - \tau_f$ breakdown stress drop
k	elastic constant of the spring (per unit fault surface)
m	mass of the spring (per unit fault surface)
$\omega_0 \equiv \sqrt{\frac{k}{m}}$	angular frequency
v_0	initial sliding speed
$x_L = \frac{\tau_u}{k}$	position of the loaded spring (with respect to its initial position $x = 0$)
s	total developed slip (namely $s = x(t_f)$)
v_{peak}	peak of the sliding speed (namely, $v_peak = x_dot(t_peak)$)
t_{peak}	instant at which v_{peak} is attained
t_f	instant at which $v \simeq 0$ is attained
γ	proportionality constant in the case of viscous friction
$\beta = \frac{\gamma}{2m}$	angular frequency in the case of viscous friction
$\omega^2 \equiv \omega_0^2 - \beta^2 = k - \frac{\gamma}{2m}$	angular frequency in the case of viscous small damping
$\Omega^2 \equiv \beta^2 - \omega_0^2$	angular frequency in the case of viscous strong damping
μ	friction coefficient
a, b, L	governing parameters of rate-and state-dependent friction
ϕ	state variable
μ_0	reference value of μ
v_*	reference value of sliding speed for RS laws (equal to the initial speed)

Table 2
Values of the parameters employed for the models investigated for Coulomb (Section 2) and viscous (Section 3) friction.

τ_u (MPa)	τ_f (MPa)	k (MPa m^{-1})	ω_0 (rad s^{-1})
17.2	15.3	10	1.26

Table 3
Values of the additional parameters required for the rate and state model (Section 4). Note that we adopt a different value of τ_f with respect to Coulomb and viscous cases (see Sections 2 and 3, respectively).

τ_f (MPa)	μ	a	b	L (m)	v_0 (ms^{-1})
31.1	0.5	0.007	0.016	$1 \cdot 10^{-5}$	$3.17 \cdot 10^{-10}$

As a typical case we consider the values of parameters given in Table 2 (and neglect the term in v_0 in Eq. (4)). From these values of k and ω_0 one has $m = 6.34 \cdot 10^6$ kg/m^2. The resulting trajectory is shown in Fig. 1. We emphasize that the perfect symmetry of the slip velocity function with respect to t_{peak} is somehow an idealization; indeed classical results of fracture mechanics and numerical models of earthquake ruptures tend to indicate more complicated and non symmetric behavior (see for instance Bizzarri, 2012a).

3. Viscous friction

In this case we consider a dynamic friction which is now not constant, but explicitly depends on the sliding speed, through a proportionality constant γ:

$$\tau_f = -\gamma \dot{x}.$$

This corresponds to a viscous behavior, where friction increases with sliding velocity. Thus, in order the have a finite slip, an initial static friction must be present, as for the Coulomb case, such that a stress drop is produced when the slip starts. In order to keep the model as simple as possible we assume that the dynamic friction $\tau_f = 0$, therfore $\Delta\tau_b = \tau_u$. Adopting the same notation and initial conditions as in the previous section one comes to the following equation of motion

$$m\ddot{x} = -k(x - x_L) - \gamma\dot{x}, \tag{6}$$

where, as before, $kx_L = \tau_u$ (Eq. (2)) is the static friction at detachment (rupture condition Eq. (1). This equation can be recast into

$$\ddot{x} + 2\beta\dot{x} + \omega_0^2(x - x_L) = 0 \tag{7}$$

with $\beta \equiv \gamma/(2m)$. The nature of solutions is determined by the value of the quantity $\omega_0 - \beta$, as described in the three following subsections.

3.1. Small damping ($\omega_0 > \beta$)

The general solution of Eq. (7) for $\omega_0 > \beta$ is

$$x(t) = e^{-\beta t}(ae^{-i\omega t} + be^{i\omega t}) + x_L,$$

where $\omega^2 \equiv \omega_0^2 - \beta^2 = k/m - (\gamma/(2m))^2$, showing an exponential damping. Imposing the initial conditions ($x(0) = 0$ and $\dot{x}(0) = v_0$) yields:

$$x(t) = e^{-\beta t}[x_S \sin(\omega t)) - x_L \cos(\omega t)] + x_L, \tag{8}$$

where $x_S \equiv (v_0 - \beta x_L)/\omega$. The dynamics is consequently damped oscillatory, and

$$\dot{x}(t) = e^{-\beta t}[(x_L\omega - \beta x_S)\sin(\omega t)) + (x_S\omega + \beta x_L)\cos(\omega t)]. \tag{9}$$

By neglecting again v_0 this takes the simpler form:

$$x(t) = x_L\left[1 - e^{-\beta t}\left(\frac{\beta}{\omega}\sin(\omega t) + \cos(\omega t)\right)\right], \tag{10}$$

and

$$\dot{x}(t) = x_L\frac{\omega_0^2}{\omega}e^{-\beta t}\sin(\omega t)). \tag{11}$$

Even for this case the derivation of s, v_{peak}, t_{peak} and t_f is straightforward. From Eqs. (10) and (11) we obtain:

$$s = \frac{\Delta\tau_b}{k}\left(1 + e^{-\frac{\beta\pi}{\omega}}\right)t_f = \frac{\pi}{\omega}$$
$$v_{peak} = \frac{\Delta\tau_b}{k}\omega_0 e^{-\frac{\beta}{\omega}\arctan(\frac{\omega}{\beta})}t_{peak} = \frac{1}{\omega}\arctan\left(\frac{\omega}{\beta}\right).$$

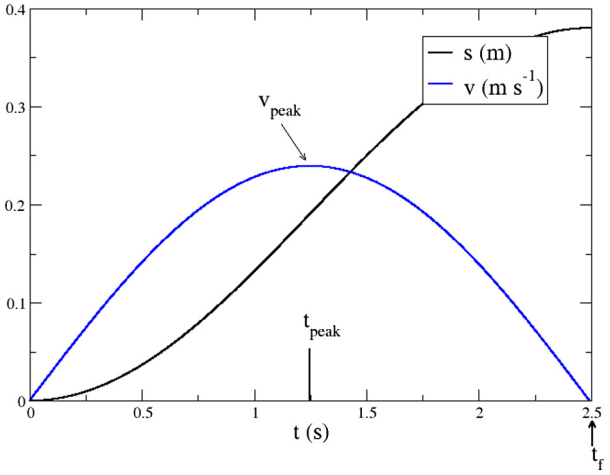

Fig. 1. Trajectory and velocity of slip motion for Coulomb friction (see the text for parameter values). Only in this figure we explicitly indicate the most relevant quantities; the peak in slip velocity (v_{peak}), its time occurrence (t_{peak}), and the total slip duration (i.e. the supprto of the slip velocity function, t_f).

It this case the relevant parameter is $\beta/\omega = \gamma/(2\sqrt{mk})$ (or equivalently ω/ω_0), and we can conclude that:

(a) The slip extension s depends on a combination of all the parameters;
(b) The slip velocity is highly asymmetric in time;
(c) The slip duration t_f only depends on ω, and not on friction;
(d) The same does not hold for t_{peak} since it depends also on β.

As an example of the resulting motion we consider the same parameters as in the previous section, Table 2, and a set of values of β in the range $\omega_0 + 0.2j\ s^{-1}$, with $j = -1, \ldots -5$. The resulting slip and velocities are shown by the upper five curves in Figs. 2 and 3, respectively. From these figures we can clearly see that the overall behavior of the system depends on the value of β; at small β it is faster, the slip reaches its final value (Fig. 2) and, correspondingly, the slip velocity goes to zero (Fig. 3).

3.2. Strong damping ($\omega_0 < \beta$)

For imaginary ω ($\omega_0 < \beta$, since, as stated above $\omega^2 \equiv \omega_0^2 - \beta^2$) the dynamics is strongly damped:

$$x(t) = e^{-\beta t}[x_S \sinh(\Omega t)) - x_L \cosh(\Omega t)] + x_L, \tag{12}$$

and the velocity is described by:

$$\dot{x}(t) = e^{-\beta t}[x_S \sinh(\Omega t)) - x_L \cosh(\Omega t)] + x_L, \tag{13}$$

where $\Omega^2 \equiv \beta^2 - \omega_0^2$. By neglecting again v_0:

$$x(t) = x_L\left[1 - e^{-\beta t}\left(\frac{\beta}{\Omega}\sinh(\Omega t) + \cosh(\Omega t)\right)\right], \tag{14}$$

and

$$\dot{x}(t) = x_L\frac{\omega_0^2}{\Omega}e^{-\beta t}\sinh(\Omega t). \tag{15}$$

Being the motion dominated by an exponential terms, slip extension is reached in infinite time. We conventionally take $1/\beta$ as a characteristic time of the slip, and we found:

$$\begin{cases} s = \frac{\Delta\tau_b}{k} & t_f = 1/\beta(\infty) \\ v_{peak} = \frac{\Delta\tau_b}{k}\omega_0 & t_{peak} = \frac{1}{\Omega}\text{atanh}(\frac{\Omega}{\beta}). \end{cases}$$

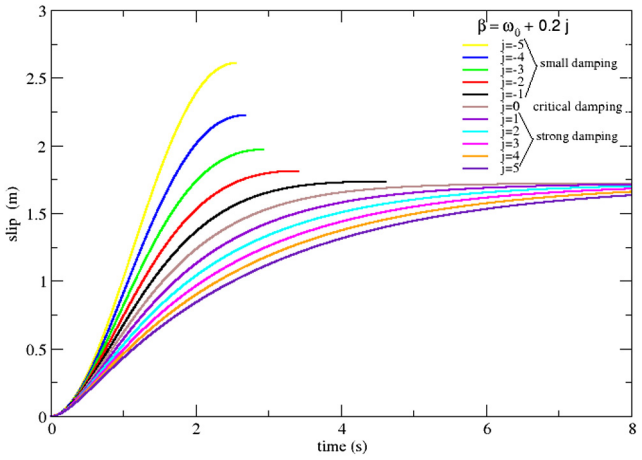

Fig. 2. Trajectories of the of slip motion in the presence of viscous damping with the parameters of Table 2 and different β. For the small damping case (negative j) slips stop when velocity drops to zero. Curves are arrested once the slip velocity comes back to zero (first five cases, pertaining to the small damping regime). Slip asymptotically reaches its final value in the other cases (critical and strong damping).

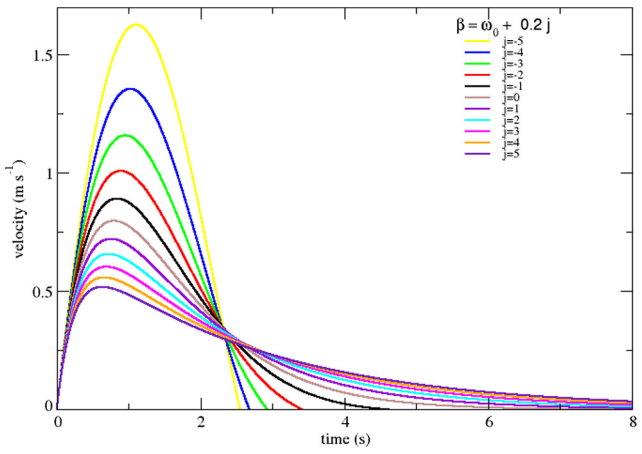

Fig. 3. Velocity for slip motion in the presence of viscous damping corresponding to Fig. 2.

Trajectories and velocities for $\beta = \omega_0 + j \cdot 0.2$, with $j = 1, 2 \ldots 5$ are shown from the lowest five curves in Figs. 2 and 3.

3.3. Critical damping ($\omega_0 = \beta$)

For $\omega = 0$ ($\beta = \omega_0$) the motion is critically damped, given by

$$x(t) = x_L(1 - e^{-\beta t}(\beta t + 1)), \tag{16}$$

and thus

$$\dot{x}(t) = x_L \beta^2 e^{-\beta t} t. \tag{17}$$

This critical case predicts that:

$$s = \frac{\Delta\tau_b}{k} \quad t_f = 1/\omega_0\,(\infty)$$
$$v_{peak} = \frac{\Delta\tau_b}{k}\omega_0 e^{-1} \quad t_{peak} = \frac{1}{\omega_0} = \frac{1}{\beta}.$$

where again we have taken $t_f = 1/\beta$. Slip and velocity for the same parameters previously adopted are shown by the middle curve in Figs. 2 and 3. This line discriminates between cases where slip reaches relatively fast its final value and cases where it asymptotically increases through time.

3.4. Viscous plus dynamic Coulomb friction

After considering the separate cases of hydrodynamic and dynamic Coulomb friction it is not difficult to see that the solutions for the case in which both frictions are present are formally identical to those encountered in the previous cases, but now $\Delta\tau_b = \tau_u - \tau_f$ with $\tau_f > 0$. Thus also the values of s and v_{peak} change accordingly.

4. Rate-and state-dependent friction laws

We now study the motion described by the equation

$$\ddot{x} + \omega_0^2(x - x_L) = -f \tag{18}$$

where the friction term $f = g\mu$ is now given by a *rate-and-state* law (μ is the friction coefficient and g is the gravity acceleration). As before $\omega_0 \equiv \sqrt{k/m}$, and $x_L = \tau_u/k$ is the initial value of the strain. We shall consider the following, canonical, formulation for rate-and-state:

$$\begin{cases} \mu = & \mu_0 + a\ln\left(\frac{v}{v_0}\right) + b\ln\left(\frac{v_0}{L}\phi\right) \\ \dot{\phi} = & 1 - \frac{v}{L}\phi, \end{cases} \tag{19}$$

where μ_0 is the reference value of the friction coefficient and $v = \dot{x}$. Namely, Eq. (19) are the Dieterich–Ruina (DR henceforth) model, which fits laboratory experiments conducted originally on bare surfaces and at relatively low sliding speed (Dieterich, 1978; Ruina, 1980). Subsequently, Marone (1998) and Mair and Marone (1999) investigated the limits of ts validity for laboratory granular fault gouge. Note that in (19) we assume that the reference value of the sliding speed v_0 – often denoted with the symbol v_* – equals the initial sliding speed $\dot{x}$. In this model a, b are the constitutive parameters accounting for the slip-hardening and slip-weakening stages of the rupture, respectively, while the third governing parameter L is the scale length over which the state variable ϕ evolves. The latter in the DR framework physically represents the average contact time of the micro-asperities populating the two sliding surfaces. Readers can refer to Section 7 of Bizzarri (2011) for a thorough review of the subject.

As for the previous cases, we shall assume that before slipping the system is performing a stationary sliding with $v = v_0$, and that the state variable has the value $\phi = L/v_0$ (that is, ϕ is on its steady state for $t \leqslant 0$). Thus when the slip starts, at $t = 0$, we have the following initial conditions

$$\mu = \mu_0$$
$$\dot{\phi} = 0.$$

In the case of Coulomb friction, previously analyzed, we assumed a slip started as soon as kx_L was larger than the friction initial value τ_u. Eq. (19) would yield in the present case the mobility stress edge $\mu_0 gm$. However we see from Eq. (19) that one has $\mu_0 gm = \tau_f$, and that the initial derivative of the friction force at $t = 0$ is:

$$\dot{\mu} = a\frac{\dot{v}}{v_0}, \tag{20}$$

that is always positive, irrespectively of the value of b. So we expect that the slip terminates immediately if $\Delta\tau_b = \tau_u - \tau_f$ is about zero. The situation is very different from the Coulomb and viscous cases. Thus we suppose that the system undergoes a sudden strain at $t = 0$ in the positive x direction, up to a certain $x_L = \tau_u/k$, and investigate

the slip properties as function of the resulting breakdown stress drop $\Delta\tau_b = kx_L - \mu gm$.

4.1. Invariant form

Before proceeding numerical computations it is important to point out that Eqs. (18) and (19) can be casted in a form invariant with respect to changes of the parameters v_0 and L. In other words, it can be shown that these parameters only set the space and time scales, that is all the trajectories obtained with different values of L and v_0 have the same shape and can be collapsed to a single one by suitable rescaling. Thus the results obtained for a couple of values (L, v_0) will hold for any couple.

The invariant form can be obtained by adopting L as unit of length and L/v_0 as unit of time, then the adimensional variables $z \equiv x/L$ for the space and $\theta \equiv v_0 t/L$ for the time (see Appendix A), obtaining (where the primes indicate the derivation with respect to θ)

$$z'' + \Omega_0^2(z - z_L) = -r \tag{21}$$

with

$$r = r_0 + \alpha \ln z' + \beta \ln \psi \tag{22}$$

and

$$\psi' = 1 - z'\psi, \tag{23}$$

where $\psi \equiv v_0\phi/L$, and $z_L \equiv x_L/L$.

In this form (Eqs. (22) and (23)) the rate-and-state law is independent on the values of L and v_0, and has just three independent parameters: r_0, α and β (for the connection of the various quantities to the original ones see Appendix A).

An invariant form is important since it allows to investigate the intrinsic properties of trajectories. In fact, once determined the solution of an invariant equation, this holds for any values of the parameters, that just affect space and time scales. To get the desired solution it is sufficient to multiply spatial and temporal values for the units corresponding to the desired parameters. On the other hand, as long as parameters appear explicitly in equations, it is difficult to know whether they just change some scale factors or affect the intrinsic nature of the motion. In the first case all trajectories can be collapsed to a single one after suitable rescaling, in the second they cannot.

Eqs. (21)–(23) can be formally integrated giving

$$z'' + \alpha \ln(1 + z') + \beta \ln(1 + e^{-z}\underline{e^z} + \psi_0) + \Omega_0^2(z - z_L) = r_0, \tag{24}$$

where $\underline{\ldots}$ stays for $\int_0^t \ldots dt'$, and ψ_0 is the initial value of ψ. This integro-differential equation contains a kernel showing explicitly that friction has a memory. Specifically it is seen that friction depends on the detailed trajectory $z(t)$ along which the integral is performed.

4.2. Numerical integration

To compute the slip trajectory under the rate-and-state friction force one has soon or later to resort to numerical integration. The numerical integration is necessary especially because of the logarithmic terms in the expression of friction. Integration of Eq. (18) has thus been performed via the Verlet algorithm (Frenkel and Smit, 2002). At the same time, in order to improve the reliability of our results we have implemented two different techniques for computing the state variable ϕ by integrating Eq. (19). The first technique (e.g. Bizzarri, 2012b) is a 4th order Runge–Kutta approximation (see e.g. Press et al., 1992), largely employed in this type of investigation. The second technique is completely novel and makes use of an explicit integral expression for ϕ, derivable from (19) (see Appendix B.1):

$$\phi(t) = e^{-x(t)/L}\left(\int_0^t e^{x(t')/L}dt' + \phi(0)\right). \tag{25}$$

From this expression a numerical algorithm can be derived (Appendix B.2) that considerably speeds up calculations with respect to the Runge–Kutta technique. In addition, we have verified in simple exactly integrable cases (consisting in imposing $v =$ const and $v = L_0/(t_0 + t)$, with L_0 and t_0 arbitrary) that it can also yield more accurate results. Anyway we have performed all computations maintaining both methods in order to compare the results.

As shown above, the equation of motion for the present case could be investigated in its invariant form, but for the sake of clarity we shall maintain the original form (18). We shall adopt the values of k and T of Table 2, thence the same values for ω and m adopted previously. The values adopted for the others parameters are shown in Table 3. As specified before, the system is supposed to undergo slow and stationary creep, such that at $t = 0$ one has $\dot{x}(0) = v_0$ and $\phi(0) = L/v_0$, moreover $\dot{\phi}(0) = 0$ and $\mu(0) = \mu_0$. With these values the stress mobility edge results $\mu_0 gm = \tau_f = 31.098$ MPa, about two times greater than the Coulomb static friction previously adopted (see Table 2).

Another crucial point is the initial value of ϕ. If it is too close to zero, the slip gives initially rise to an increase of friction. In order to have instability the initial value must be high (physically, since ϕ represents the average contact time of micro-asperity contacts in the DR model, this indicates that the fault has been locked for a long time and thus that it is prone to rupture). A commonly adopted choice is $\phi(t = 0) = L/v_0$, which is the stationary value exponentially attained in a motion at constant speed v_0. For the adopted parameters we have $\phi(0) = 31.5 \cdot 10^3$ s.

4.3. Slip properties

In this section we investigate how the dependence of the main slip properties (again, extension, s, duration, t_f, peak velocity, v_{peak}, its instant, t_{peak}) depend on the value of the initial stress τ_u.

Fig. 4 shows the slip trajectories for different values of τ_u. It is seen that for large $\Delta\tau_b = \tau_u - \tau_f$, slips start almost immediately and all have about the same duration, but when $\Delta\tau_b$ becomes small, the motion displays a creeping (or preslip) phase that gets longer the smaller is $\Delta\tau_b$ (Fig. 5). After this phase the macroscopic sliding starts. In this range of $\Delta\tau_b$ the peak velocity decreases. We recall that according to Eq. (20) we expect a strong inhibition of motion when τ_u approaches τ_f. Fig. 6 displays the velocity curves for the different slips on double logarithmic scale. It shows that v_{peak} actually decreases with decreasing $\Delta\tau_b$. This results is also in agreement with findings from extended fault model (e.g. Bizzarri, 2012a) and with the laboratory evidences from expansion of pure mode II crack (Ohnaka et al., 1987).

4.4. Slip extension and peak velocity

The dependence of the slip extension s and peak velocity v_{peak} on the initial stress τ_u are reported in Fig. 7. It is seen that both v_{peak} and s scale linearly with τ_u:

$$s \simeq a_s \tau_u$$
$$v_{peak} \simeq a_v \tau_u,$$

where a_s and a_v are constant. It is interesting to point out that the same linear dependence was found for the Coulomb friction law (Section 2). In that case the proportionality coefficients were

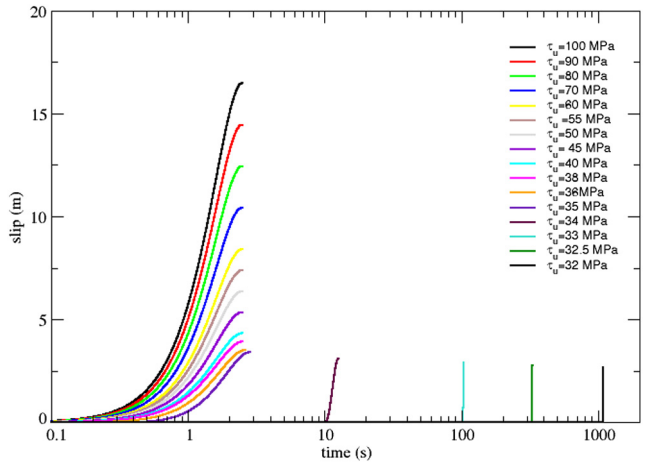

Fig. 4. Slip trajectory in the presence of rate-and-state friction (Eq. (19)), for different values of the initial stress reported in the legend. For values approaching the mobility edge μgm, slips display a creeping phase before to slide macroscopically much less than normal slips. As for Fig. 2, also in this case curves are arrested when slip velocity is zero.

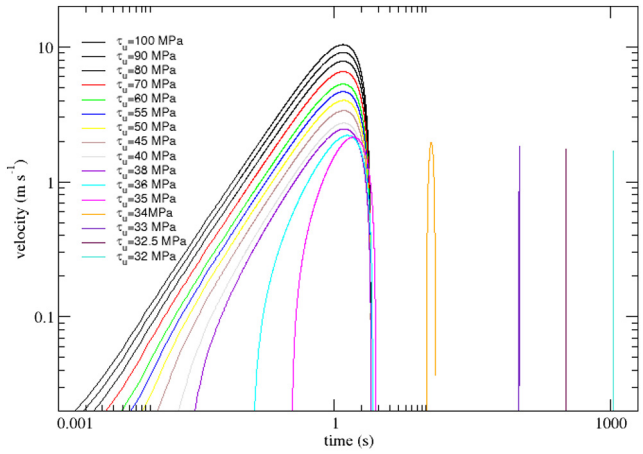

Fig. 6. Velocity trajectory, corresponding to slip curves reported in Figs. 4 and 5, in the presence of rate-and-state friction (Eq. (19)) for different values of the initial stress (see text). As long as τ_s approaches μgm the rupture time increases; the velocity always comes back to zero after its peak The pulse seems a vertical line only because of the logarithmic scale and the absolute values of rupture times.

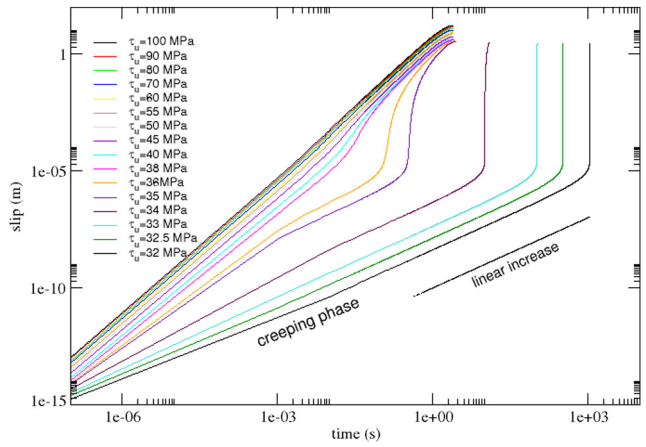

Fig. 5. The same as Fig. 4, but now in logarithmic scale. It is clear that the creeping phase is characterized by a linear increase of slip with time. For values approaching the mobility edge μgm, slips display a creeping phase before to slide macroscopically (nearly vertical lines).

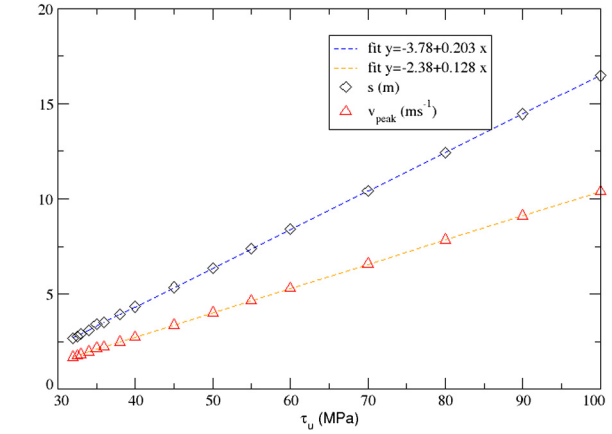

Fig. 7. Slip extension (s) and peak velocity (v_{peak}) for different values of the initial stress τ_s, in the presence of rate-and-state friction, Eq. (19) (see Section 4.4 for details). Dashed lines indicates linear fits for the data for s and v_{peak}; equations are reported in the legend. In this series of numerical experiments we adopted $\omega = 1.26$ rad s^{-1} and $k = 10^7$ MPa m^{-1}.

$a_s = 2/k = 0.2$ m MPa^{-1} for s and $a_v = (m\omega_0)^{-1} = 0.125$ m (MPa s)$^{-1}$ for v_{peak}. By fitting data of Fig. 5 we obtained for rate-and-state:

$$a_s = 0.203 \text{ mMPa}^{-1}$$
$$a_v = 0.128 \text{ mMPa}^{-1}\text{ s}^{-1}.$$

Notably, these values are within numerical errors, the same values pertaining to the Coulomb case. This suggests that for RS friction we have the same dependence on k and ω_0 observed in the Coulomb case. To test this hypothesis we have computed the slips properties for different ω_0 and k. Indeed, from the obtained results we observed that the dependence of v_{peak} and s on the system parameters are the same for Coulomb and rate-and-state friction. However the linear fits indicate that both s and $v_{peak} \to 0$ for $\tau_u \to 1.86$ MPa, a value much lower than τ_f. So we guess that a sudden faster-than-linear drop to zero of both quantities must be expected for values of $\Delta\tau_b$ smaller than the one investigated, but still positive.

In the pure viscous case (see Section 3) s and v_{peak} do not depend on $\Delta\tau_b$, since in that case $\tau_u = 0$, but in any case $a_s \propto 1/k$ for small damping. For large or critical damping the slip is exponentially infinite, but with a prefactor which depends on τ_u again as $1/k$. Concerning $v_{peak}, a_v = \omega_0/k$ for small and strong damping, while there is an extra $1/e$ factor in the critical case. When both Coulomb and viscous friction are present the related dependence on $\Delta\tau_b$ is recovered.

Thus we conclude that at least in the considered range of $\Delta\tau_b$, the dependence of v_{peak} and s on the system parameters *are the same for Coulomb, viscous, and rate-and state friction laws*. Because of the invariance of the rate-and-state law, demonstrated in Section 4.1, this holds for any value of L and v_0.

4.5. Slip duration and peak velocity instant

In the Coulomb case the slip duration was independent of $\Delta\tau_b$. In the present case it is the same for large values of $\Delta\tau_b$. It remains now to investigate if the duration changes following ω_0^{-1} as in the Coulomb and small damping viscous cases, or other laws. For $\Delta\tau_b$ approaching 0, the slip duration increases due to the appearance of the creeping phase. However, if one looks at the duration of

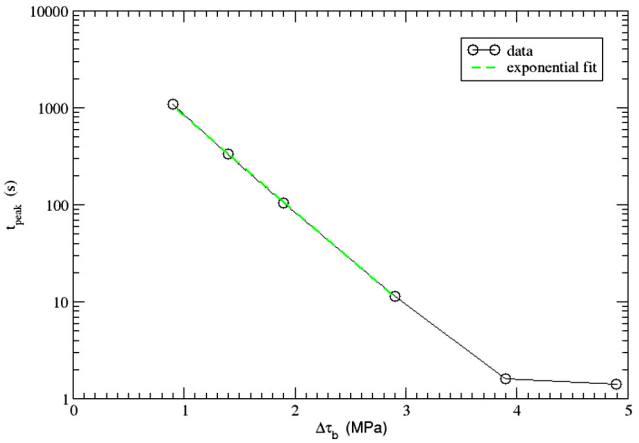

Fig. 8. Rate and state friction law: the instant of the peak velocity for the creeping slips tends to increase exponentially when $\tau_u \to \tau_f$. The green line is a fit $\propto \exp^{-(\tau_b/\tau_0)}$ with characteristic stress $\tau_0 = 0.88$ Mpa (note the logarithmic scale on the ordinate axis).

the macroscopic slip only (the almost vertical part of trajectories in Fig. 5) one sees that it is the same as for the normal slips.

As concerned t_{peak}, the time at which v_{peak} is reached, it is independent of τ_u for the regular slips, that is as far as $\Delta\tau_b$ is large enough. It can be useful to remind that it is the same for the Coulomb and viscous friction, but following different laws. On the contrary, creeping slips display an exponential increase for decreasing $\Delta\tau_b$ as $t_{peak} \approx \exp(\tau_u/\tau_0)$ (Fig. 8), where $\tau_0 = 0.88$ MPa is a fitting characteristic stress. Remarkably, this value is not far from ω^{-1}. At the same time, if one considers only the macroscopic part of the slip, that follows the creeping, and sets the origin of time at its beginning, one finds again $t_f \simeq \pi/\omega_0$ and $t_{peak} \simeq \pi/2\omega_0$.

5. Velocity spectrum

An interesting issue consists in the spectral content $S(\nu)$ of the sliding speed, defined as $S(\nu) = |\hat{v}(\nu)|$ where $\hat{v}$ is the Fourier transform of v:

$$\hat{v}(\nu) = \int_0^{t_f} e^{-2i\pi\nu t}\dot{x}(t)dt. \tag{26}$$

Note that the boundaries of integration have been reduced to the support of the function v.

5.1. Coulomb

For the case of Coulomb friction (Eq. (5)) this is extremely simple since the only characteristic frequency is $\nu_0 \equiv \omega_0/(2\pi)$ (here and in the following we drop terms in ν_0 in the expressions of velocity, namely the second term in the r.h.s member of equation (5)):

$$\hat{v}(\nu) = \frac{\Delta\tau_b}{k}\frac{\nu_0^2\left(1+e^{i\pi\frac{\nu}{\nu_0}}\right)}{\nu^2-\nu_0^2},$$

or

$$\hat{v}(\nu) = \frac{\Delta\tau_b}{k}\frac{1+e^{i\pi\zeta}}{\zeta^2-1},$$

where $\zeta \equiv \nu/\nu_0$. The spectrum increases hyperbolically around the singularity at ν_0, with an amplitude directly proportional to the stress drop. The form of the numerator shows a superimposition of oscillations at frequency ν_0.

5.2. Viscous

In the case of viscous friction the process is dominated by the exponential and we expect to find a long Lorentzian tail $S(\nu) \simeq \nu^{-2}$. In fact from Eq. (26), in the case of small damping (equation (11)), one has:

$$\hat{v}(\nu) = x_L\frac{\omega_0^2}{\omega}\int_0^{t_\nu} e^{-i2\pi\nu t}e^{-\beta t}\sin(\omega t)dt$$
$$= \frac{x_L}{2i}\frac{\omega_0^2}{\omega}\int_0^{\pi/\omega} e^{-\{\beta+i(2\pi\nu-\omega)\}t} - e^{-\{\beta+i(2\pi\nu+\omega)\}t}dt$$

from which one obtains

$$\hat{v}(\nu) = -x_L\frac{\pi\nu e^{-\frac{\beta\pi}{\omega}}}{\omega}\frac{\omega_0^2 e^{-\frac{i2\pi^2\nu}{\omega}}}{(\beta+2i\pi\nu)^2+\omega^2}.$$

As expected the spectrum is dominated by a ν^{-2} tail, but in this case we do no expect harmonics from the numerator.

For the strongly damped case (Eq. (15))

$$\hat{v}(\nu) = -x_L\frac{\omega_0^2}{(\beta+2i\pi\nu)^2-\Omega^2}, \tag{27}$$

that is again no harmonics and an inverse square tail but flattening at high frequencies.

Finally, the viscous critical case (Eq. (17)) has also a simple spectrum given by:

$$\hat{v}(\nu) = -x_L\frac{\omega_0^2}{(\omega_0+2\pi i\nu)^2}, \tag{28}$$

or

$$\hat{v}(\nu) = -x_L\frac{1}{(1+i\zeta)^2}$$

where again $\zeta \equiv 2\pi\nu/\omega_0$.

5.3. Rate and state

The spectrum for the DR law has been computed numerically for the cases investigated in Section 4.3. The resulting curves are shown in Fig. 9 where one can see that at low frequencies one has again

$$S(\nu) \approx \nu^{-2}$$

which is similar to the viscous cases. Moreover, one can see that for the creeping sleeps the system characteristic frequency $\nu_0 = \omega_0/2\pi$ superimposes to the spectrum with its harmonics. Actually this is expected to occur also for the regular slips.[1].

6. Conclusions

In the literature (Bizzarri, 2011 and references therein) it has been shown that during the coseismic stage of the rupture – i.e, the time window when shear traction is released and seismic wave are excited, rate–and state–dependent friction laws (RS) (Ruina, 1983) yield similar results with respect to those predicted by slip-weakening friction law (Andrews, 1976), provided that the governing parameters are properly selected. This holds for the traction behavior on the fault (i.e. the so-called slip-weakening phase diagram), for the rupture speed (see also Okubo, 1989), for the spectrum energy density and also for the synthetic seismograms, i.e., for the time evolution of the ground motions (out of the fault

[1] The discrete Fourier transform of regular slips, computed numerically and reproduced in the picture, is not able to show this feature because of the too large sampling frequency $\delta\nu = 1/t_f$. Since $t_f \approx \pi/\omega_0$, then $\delta\nu \simeq 2\nu_0 > \nu_0$.

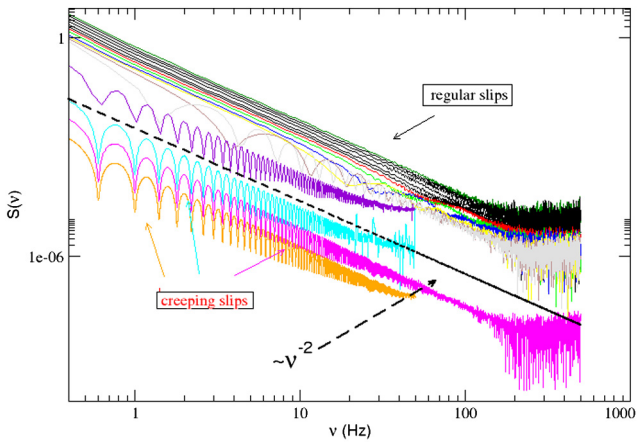

Fig. 9. Velocity spectrum for slip motion subjected to rate-and-state friction, Eq. (18), for different values of the initial stress (see Section 5).

surface; see again Bizzarri (2011)). The comparison between RS and more simple, let say "classical" rheologic behavior, such as Coulomb friction (which prescribes a constant level of dynamic friction after the rupture onset) or the viscous friction (where the excited, rate–and state–dependent resistance linearly depends on sliding speed) +was missing and this work fills this gap.

In the present paper, by considering analytical solutions for a single spring-slider analog fault model, we have scrutinized the properties of the solutions of the equation of motions for different rheologies. The model adopted here, basically a damped harmonic oscillator, has been the subject of a quite vast body of literature and it has been employed to describe many aspects of faulting mechanisms during the whole life of a fault system (namely, the seismic cycle). Readers can refer to Gu et al. (1984) and to Bizzarri (2012c) for the general framework and for several examples of seismological applications. In details, we have considered the most simple Coulomb friction (Section 2), the case of viscous friction (Section 3) and a more elaborated version of the rate-and state-dependent friction, the Dieterich–Ruina model (Section 4). By comparing the different solutions we obtain, we are able to highlight some general features, as discussed previously.

There is no reason to overemphasize that the present comparison holds only within the coseismic stage of the rupture, where the loading rate (of tectonic origin) can be safely neglected in the equation of motion, and where we do not need any re-strengthening mechanism (which indeed is a feature of the RS law only). Indeed, it is important to remark that this is the only physical assumption we made in the present model. To summarize the main conclusions of the present work we can state what it follows.

1. *Slip extension s* The slip extension results proportional only to the difference $\Delta\tau_b$ between the initial stress τ_u and the friction τ_f, and inversely proportional to the spring constant *k for all the investigated friction laws*, although for RS non obvious additive constants ($e^{-\beta\pi/\omega}$) appear. The mass is irrelevant.
2. *Maximum slip velocity* v_{peak} The maximum velocity reached during the slip is again proportional to $\Delta\tau_b/k$ but through ω_0. This holds for Coulomb and viscous cases and, from our numerical evidences, for rate-and-state. This result is in agreement with the laboratory inferences by Ohnaka et al. (1987), which predicts a direct proportionality between s and $\Delta\tau_b$, $v_{peak} \simeq v_r\Delta\tau_b/G$, i.e., through a proportionality constant which depends on the speed of the rupture, v_r, and the rigidity of the elastic medium, G. A similar relation emerges from the analytical solutions of a non spontaneous model (i.e. with prior-imposed rupture speed) of a rupture on a fault where the friction is assumed to linearly decrease with increasing distance from the nucleation point (Palmer and Rice, 1973, cfr. also Eq. (14) of Bizzarri (2012a)). Our general result ($s \approx \Delta\tau_\beta/k$) can not obviously contain any reference to the rupture speed v_r (as the results mentioned above), due to the 1-D nature of our analog fault model, in which we have only the dependence on time and we do not have any information regarding the spatial domain (remember that our simple spring-slider system is point-like) and thus on the rupture front and velocity.
3. *Slip duration* t_f The slip duration (i.e. the time during which the slip increases or, equivalently, the support of the slip velocity function) is proportional to $\omega_0^{-1} = \sqrt{m/k}$ for Coulomb and for viscous rheology, in the small and critical damping cases. For strong damping $t_f = \infty$, since it slows down exponentially, with a characteristic time $1/\beta$, which also is the t_f of the critical case, where $\beta = \omega_0$. We point out that in any case there is no dependence on $\Delta\tau_b$. For the investigated cases of rate-and-state t_f is also found independent of $\Delta\tau_b$ and close to π/ω_0. This holds also for the macroscopic slips following a long creeping, if one considers the end of the preslip as the origin of times.
4. *Time of the peak velocity* t_{peak} This quantity seems the more distinctive among the different friction laws. Indeed, t_{peak} controls the different phases of the dynamic motion; in the interval $[0, t_{peak}]$ we have the acceleration phase, while in $(t_{peak}, t_f]$ the fault experiences its decelerating stage. Our results thus indicate that the acceleration and deceleration durations depend on the adopted rheologic model of the fault. The $\pi/(2\omega_0)$ dependence for Coulomb is replaced by $\omega^{-1}\arctan(\omega/\beta)$ for small damping and the analogous law for strongly damping. For critical damping one has $t_{peak} = \omega_0^{-1} = \beta^{-1}$. The independence on $\Delta\tau_b$ is observed also in the rate and state case, where also $t_{peak} \simeq \pi/2\omega_0$, but only for large values of $\Delta\tau_b$. For τ_u approaching the mobility stress (recall that the mobility stress edge is $\mu_0 gm$ for rate-and-state; see Section 4) we observe $t_{peak} \approx \exp(\tau_u/\tau_0)$, with τ_0 a fitting constant apparently close to ω_0^{-1} (see Fig. 8). Nevertheless, the velocity peak is reached about $\pi/2\omega_0$ after the preslip end.
5. *Velocity spectrum* $S(v)$ The spectrum of velocity for Coulomb is singular at $v_0 = \pm\omega_0/(2\pi)$, with a v^{-1} decay. For viscous damping it displays long $\simeq v^{-2}$ tails. The same holds for rate-and-state. In addition, every time the slip duration t_f is finite, harmonics of the fundamental frequency (that is ω_0 for Coulomb and rate-and-state, ω for small viscous damping) appear. Just for comparison, the modified Yoffe function, often employed as source time function in kinematic inversion (Tinti et al., 2006, and references cited therein) predicts a similar fall-off at high frequencies (see Fig. 3 of Bizzarri, 2012a).

All the above mentioned results are resumed in the synoptic table below, where we have generalized those for the viscous case to the additional presence of dynamic Coulomb friction τ_f, discussed in Section 3.4. We do not have explicit forms for the rate-and-state t_f and t_{peak}, although some guesses have been done. (see Table 4).

Appendix A

The invariant form discussed in Section 4.1 can be obtained by adopting L as unit of length and L/v_0 as unit of time, then the adimensional variables $z \equiv x/L$ and $\theta \equiv v_0 t/L$ for space and time, respectively. With the adoption of these variables, by multiplying Eq. (18) by L/v_0^2 one obtains

Table 4
Dependences of the main observables on the parameters of the model in the different rheologic cases we considered in the present work. v is the frequency, $S(v)$ is the velocity spectrum and the other quantities are tabulated in Table 1.

Type of rheology	s	v_{peak}	t_f	t_{peak}	high frequency fall-off of $S(v)$
Coulomb (Section 2)	$\frac{2\Delta\tau_b}{k}$	$\frac{2\Delta\tau_b\omega_0}{k}$	$\frac{\pi}{\omega_0}$	$\frac{\pi}{2\omega_0}$	$\simeq (v^2 - v_0^2)^{-1}$ (+harmonics)
Viscous – Small damping (Section 3.1)	$\frac{\Delta\tau_b}{k}\left(1 + e^{-\frac{\beta\pi}{\omega}}\right)$	$\frac{\Delta\tau_b\omega}{k} e^{-\frac{\beta}{\omega}} \cdot \arctan(\frac{\omega}{\beta})$	$\frac{\pi}{\omega}$	$\frac{1}{\omega}\arctan\left(\frac{\omega}{\beta}\right)$	$\simeq v^{-2}$ (+harmonics)
Viscous – Strong damping (Section 3.2)	$\frac{\Delta\tau_b}{k}$	$\frac{\Delta\tau_b\omega_0}{k}$	$\beta^{-1}\,(\infty)$	$\frac{\arctan\left(\frac{\omega}{\beta}\right)}{\beta}$	$\simeq v^{-2}$
Viscous – Critical (Section 3.3)	$\frac{\Delta\tau_b}{k}$	$\frac{\Delta\tau_b\omega_0}{ke}$	$\omega_0^{-1} = \beta^{-1}$	$\omega_0^{-1} = \beta^{-1}$	$\simeq v^{-2}$
Rate and state (Section 4)	$\frac{2\Delta\tau_b}{k}$+const	$\frac{2\Delta\tau_b}{m\omega_0}$+const	$\simeq \frac{\pi}{\omega_0}$	$\simeq \frac{\pi}{2\omega_0}$	$\simeq v^{-2}$ (+harmonics)

$$\frac{d^2z}{d\theta^2} + \Omega_0^2(z - z_L) = -r \tag{A-1}$$

where

$$\Omega_0 \equiv \frac{L}{v_0}\omega_0$$

is the adimensional angular frequency and

$$r \equiv f\frac{L}{v_0^2}$$

is the adimensional friction stress per unit mass.

The expression of f (recall that $f = g\mu(v, \phi)$) is also transformed. One can rewrite the term $v/v_0 = \dot{x}/v_0$ in terms of the new length and time units by multiplying both numerator and denominator by $L/(L/v_0)$ thus obtaining

$$v/v_0 = \frac{v}{L}\frac{L}{v_0}\Big/\frac{v_0}{L}\frac{L}{v_0} = \frac{dz}{d\theta}\Big/1.$$

In addition one can define the adimensional state $\simeq v^{-2}$ variable

$$\psi = \frac{v_0}{L}\phi,$$

and turn in a similar fashion the evolution Eq. (19) into

$$\dot{\phi} = \frac{d\psi}{d\theta} = 1 - \frac{v}{L}\phi = 1 - \frac{dz}{d\theta}\psi$$

thus obtaining, by indicating $d/d\theta$ with a prime, $'$,

$$\mu = \mu_0 + a\ln z' + b\ln\psi$$

and

$$\psi' = 1 - z'\psi,$$

By setting $\mu_0 gL/v_0 = r_0, agL/v_0 = \alpha$ and $bgL/v_0 = \beta$ one has finally the set of equations

$$z'' + \Omega_0^2(z - z_L) = -r \tag{A-2}$$

with

$$r = r_0 + \alpha\ln z' + \beta\ln\psi \tag{A-3}$$

with

$$\psi' = 1 - z'\psi, \tag{A-4}$$

which are independent of the values of L and v_0.

Appendix B

B.1. Integration of the state variable

Expression (25) derives by the direct integration of the second of Eq. (19). To see this let us notice that this equation can be rewritten as

$$\dot{\phi} + \frac{\dot{x}}{L}\phi = 1, \tag{B-1}$$

and that the left hand side member of the latter can be written as an exact differential. In fact from the identity

$$\frac{1}{f}\frac{d(f\phi)}{dt} = \dot{\phi} + \frac{\dot{f}}{f}\phi, \tag{B-2}$$

if we set $\dot{f}/f = \dot{x}/L$, so that

$$f(t) = f(0)e^{x(t)/L}. \tag{B-3}$$

then the l.h.s. member of (B-2) equals that of (B-1), which therefore sounds now

$$\frac{1}{f}\frac{d(f\phi)}{dt} = 1$$

from which

$$d(f\phi) = f dt,$$

that can be integrated to yield

$$f(t)\phi(t) - f(0)\phi(0) = \int_0^t f(t')dt'.$$

From the above equation we can then obtain an expression for $\phi(t)$:

$$\phi(t) = \frac{1}{f(t)}\left(f(0)\phi(0) + \int_0^t f(t')dt'\right).$$

By using f given by (B-3) one finally gets Eq. (25) (note that $f(0)$ is irrelevant).

B.2. Numerical iteration

By discretizing time into intervals of width δt and by indicating with the subscript n the quantities at time $t_n = n\delta t$, it is easy to see that ϕ can be computed recursively from the above equation. In fact we have

$$\phi_n = e^{-x_n/L}(I_n + \phi_0) \tag{B-4}$$

where

$$I_n = \delta t\sum_{i=1}^{n} e^{x_i/L}.$$

By noticing that in the same way

$$I_{n+1} = \delta t\sum_{i=1}^{n+1} e^{x_i/L}$$

one can write recursively

$$I_{n+1} = I_n + \delta t\exp(x_{n+1}/L). \tag{B-5}$$

One can use this equation to derive a similar recursion for ϕ_{n+1}. By using the fact that $x_n = \sum_{i=1}^{n} \delta x_n$ one can write from (B-4) and from (B-5)

$$\phi_{n+1} = e^{-x_{n+1}/L}(I_{n+1} + \phi_0) = e^{-(x_n+\delta x_{n+1})/L}\left(I_n + \delta t e^{x_{n+1}/L} + \phi_0\right)$$

from which

$$\phi_{n+1} = e^{-\delta x_{n+1}/L}\left(e^{-x_n/L}(I_n + \phi_0) + \delta t e^{\delta x_{n+1}/L}\right)$$

and thus finally

$$\phi_{n+1} = e^{-\delta x_{n+1}/L}\phi_n + \delta t. \tag{B-6}$$

This recursive algorithm considerably speeds up calculations with respect to the Runge–Kutta technique. In addition, we have verified in simple exactly integrable cases (with $v =$ const and $v = L_0/(t_0 + t)$, where L_0 and t_0 are arbitrary constants) that it also yields more accurate results. Anyway we have performed all computations maintaining both methods in order to compare the results.

It is important to emphasize that our recursive method prescribes a constant time step, δt. This is not problematic, since we consider here only the coseismic stage of the motion, so that the auto-adaptive RK method employed to solve seismic cycle, e.g. Bizzarri (2012c) and references cited therein-would be useless.

We can see that the algorithm is consistent with Eq. (19) by going back. From Eq. (B-6) one has

$$\phi_{n+1} - \phi_n = (e^{-\delta x_{n+1}/L} - 1)\phi_n + \delta t$$

that by expanding in a Taylor series the function $e^{-\delta x_{n+1}}/L$ to the first order in δt yields

$$\phi_{n+1} - \phi_n \approx -\frac{\delta x_{n+1}}{L}\phi_n + \delta t.$$

By dividing it by δt

$$\frac{\phi_{n+1} - \phi_n}{\delta t} \approx -\frac{\delta x_{n+1}}{\delta t}\frac{1}{L}\phi_n + 1$$

and by taking the limit $\delta \to 0$ one gets

$$\dot{\phi} = 1 - \frac{\dot{x}}{L}\phi$$

c.d.d.

References

Andrews, D., 1976. Rupture velocity of plane strain shear cracks. J. Geophys. Res. 81, 5679–5687.

Annunziata, A., Baldassarri, A., Dalton, F., Gnoli, A., Petri, A. 2016. Scaling breakdown and friction weakening in critical granular flow. in preparation.

Baldassarri, A., Colaiori, F., Castellano, C., 2003. Average shape of a fluctuation: universality in excursions of stochastic processes. Phys. Rev. Lett. 90.

Bizzarri, A., 2011. On the deterministic description of earthquakes. Rev. Geophys. 49, RG3002.

Bizzarri, A., 2012a. Analytical representation of the fault slip velocity from spontaneous dynamic earthquake models. J. Geophys. Res.: Solid Earth 117, B06309.

Bizzarri, A., 2012b. Rupture speed and slip velocity: what can we learn from simulated earthquakes? Earth Plan. Sci. Lett, 196–203.

Bizzarri, A., 2012c. What can physical source models tell us about the recurrence time of earthquakes. Earth Sci. Rev 115, 304–318.

Dieterich, J.H., 1978. Time-dependent friction and the mechanics of stick slip. Pure Appl. Geophys. 116, 790–806.

Frenkel, D., Smit, B., 2002. Understanding Molecular Simulations. Academic Press, San Diego.

Gu, J.C., Rice, J., Ruina, A.L., Tse, S.T., 1984. Slip motion and stability of a single degree of freedom elastic system with rate and state dependent friction. J. Mech. Phys. Solids 32, 167–196.

Kostrov, B.V., 1974. Crack propagation at variable velocity. J. Appl. Math. Mech. 38, 551–560.

Mair, K., Marone, C., 1999. Friction of simulated fault gouge for a wide range of velocities and normal stresses. J. Geophys. Res 104, 28899–28914.

Marone, C., 1998. Laboratory-derived friction laws and their application to seismic faulting. Ann. Rev. Earth Planet. Sci. 26, 643–696.

Ohnaka, M., Kuwahara, Y., Yamamoto, K., 1987. Constitutive relations between dynamic physical parameters near a tip of the propagating slip zone during stick-slip shear failure. Tectonophysics 144, 109–125.

Okubo, P.G., 1989. Dynamic rupture modeling with laboratory-derived constitutive relations. J. Geophys. Res.: Solid Earth 94, 12321–12335.

Palmer, A.C., Rice, J.R., 1973. The growth of slip surfaces in the progressive failure of over-consolidated clay. Proc. R. Soc. London, A 332, 527–548.

Press, W.H., Teukolsky, S.A., Vetterling, W.T., Flannery, B.P., 1992. Numerical Recipes in C. Cambridge University Press, New York, NY.

Rice, J.R., Tse, S.T., 1986. Dynamic motion of a single degree of freedom system following a rate and state dependent friction law. J. Geophys. Res. 91, 521–530.

Ruina, A.L., 1980. Friction Laws and Instabilities: A Quasistatic Analysis of Some Dry Frictional Behavior. Boston Univ., Providence R.I. (Ph. D. Thesis).

Ruina, A.L., 1983. Friction laws and instabilities: a quasistatic analysis of some dry frictional behavior. J. Geophys. Res. 88, 10359–10370.

Tinti, E., Fukuyama, E., Piatanesi, A., Cocco, M., 2006. A kinematic source time function compatible with earthquake dynamics. Bull. Seismol. Soc. Am. 95, 1211–1223.